AD-A142 332 GRATING LOBE CHARACTERISTICS OF ARRAYS WITH UNIFORMLY 1/1
ILLUMINATED CONTIGUOUS SUBARRAYS(U) ROME AIR
DEVELOPMENT CENTER GRIFFISS AFB NY R J MAILLOUX DEC 83
UNCLASSIFIED RADC-TR-83-290 F/G 9/5 NL

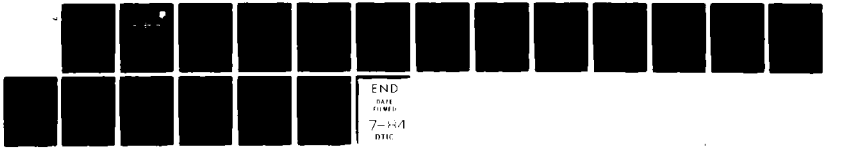

END
DATE FILMED
7-84
DTIC

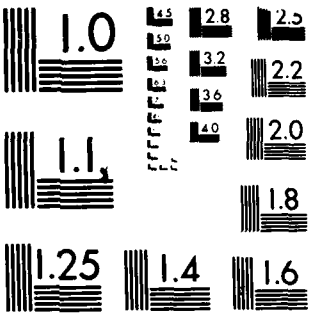

(12)

RADC-TR-83-290
In-House Report
December 1983

GRATING LOBE CHARACTERISTICS OF ARRAYS WITH UNIFORMLY ILLUMINATED CONTIGUOUS SUBARRAYS

Robert J. Mailloux

ROME AIR DEVELOPMENT CENTER
Air Force Systems Command
Griffiss Air Force Base, NY 13441

This report has been reviewed by the RADC Public Affairs Office (PA) and is releasable to the National Technical Information Service (NTIS). At NTIS it will be releasable to the general public, including foreign nations.

RADC-TR-83-290 has been reviewed and is approved for publication.

APPROVED: John K. Schindler

JOHN K. SCHINDLER
Chief, Antennas & RF Components Branch
Electromagnetic Sciences Division

APPROVED: Allan C. Schell

ALLAN C. SCHELL
Chief, Electromagnetic Sciences Division

FOR THE COMMANDER: John A. Ritz

JOHN A. RITZ
Acting Chief, Plans Office

If your address has changed or if you wish to be removed from the RADC mailing list, or if the addressee is no longer employed by your organization, please notify RADC (EEAA), Hanscom AFB MA 01731. This will assist us in maintaining a current mailing list.

Do not return copies of this report unless contractual obligations or notices on a specific document requires that it be returned.

Unclassified
SECURITY CLASSIFICATION OF THIS PAGE (When Data Entered)

REPORT DOCUMENTATION PAGE		READ INSTRUCTIONS BEFORE COMPLETING FORM
1. REPORT NUMBER RADC-TR-83-290	2. GOVT ACCESSION NO. AD-A142	3. RECIPIENT'S CATALOG NUMBER 332
4. TITLE (and Subtitle) GRATING LOBE CHARACTERISTICS OF ARRAYS WITH UNIFORMLY ILLUMINATED CONTIGUOUS SUBARRAYS		5. TYPE OF REPORT & PERIOD COVERED In-House 6. PERFORMING ORG. REPORT NUMBER
7. AUTHOR(s) Robert J. Mailloux		8. CONTRACT OR GRANT NUMBER(s)
9. PERFORMING ORGANIZATION NAME AND ADDRESS Rome Air Development Center (EEA) Hanscom AFB Massachusetts 01731		10. PROGRAM ELEMENT, PROJECT, TASK AREA & WORK UNIT NUMBERS 61102F 2305J303
11. CONTROLLING OFFICE NAME AND ADDRESS Rome Air Development Center (EEA) Hanscom AFB Massachusetts 01731		12. REPORT DATE December 1983 13. NUMBER OF PAGES 16
14. MONITORING AGENCY NAME & ADDRESS(if different from Controlling Office)		15. SECURITY CLASS. (of this report) Unclassified 15a. DECLASSIFICATION DOWNGRADING SCHEDULE

16. DISTRIBUTION STATEMENT (of this Report)

Approved for public release; distribution unlimited.

17. DISTRIBUTION STATEMENT (of the abstract entered in Block 20, if different from Report)

18. SUPPLEMENTARY NOTES

19. KEY WORDS (Continue on reverse side if necessary and identify by block number)

Grating lobes
Antenna arrays
Subarrays

20. ABSTRACT (Continue on reverse side if necessary and identify by block number)

This report presents simple approximate formulas and generalized curves to simplify evaluation of the grating lobe levels of various kinds of contiguous subarrays with uniform illumination within each subarray. The cases considered include phase quantization caused by discrete phase shifters, amplitude taper at subarray input ports, and time delay at the subarray input ports. Also, the work is generalized to include certain cases of quantized phase or time delay at the input ports in addition to amplitude taper at subarray input ports.

DD FORM 1 JAN 73 1473 EDITION OF 1 NOV 65 IS OBSOLETE

Unclassified
SECURITY CLASSIFICATION OF THIS PAGE (When Data Entered)

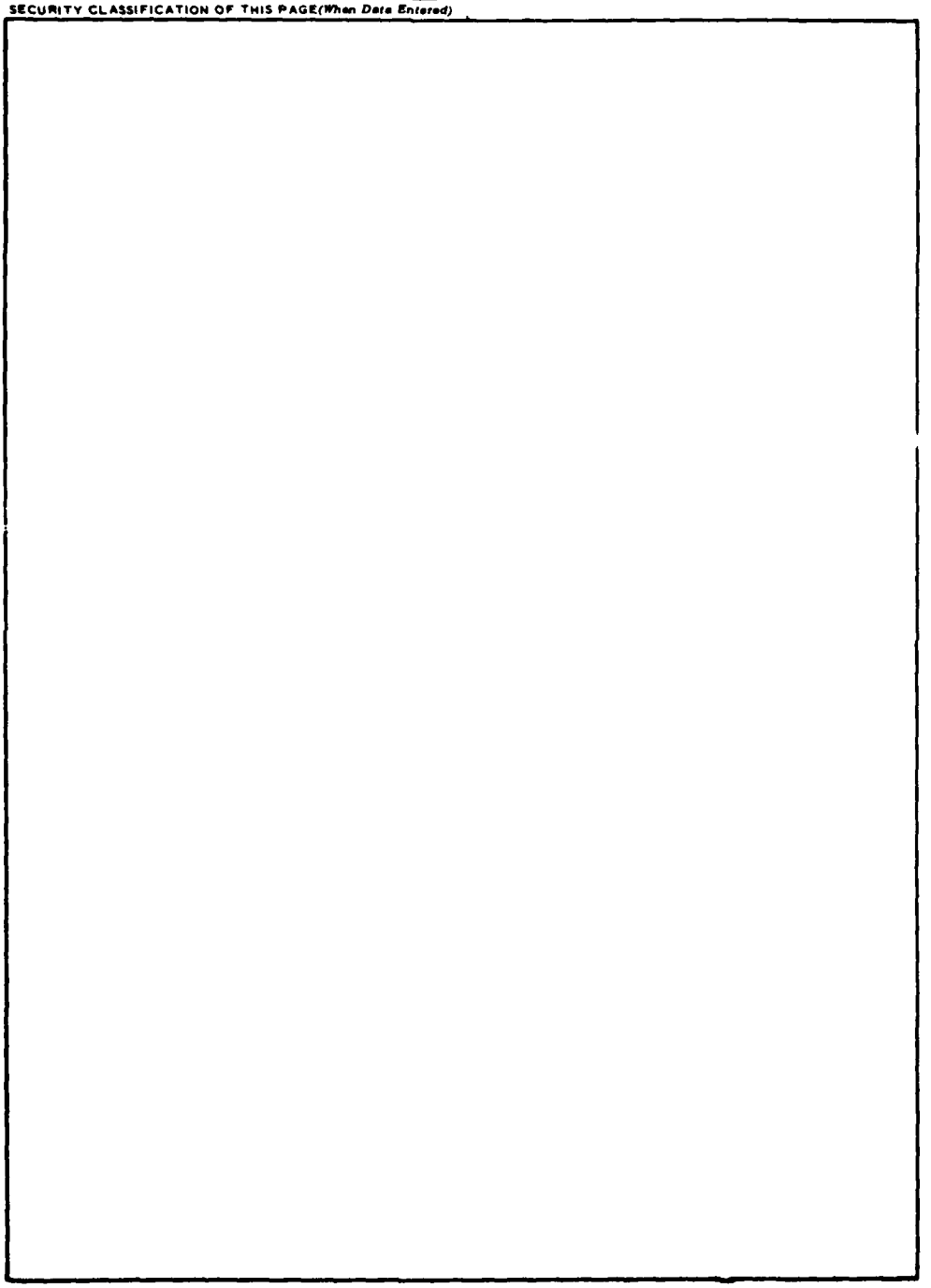

A1

Contents

Illustrations

Grating Lobe Characteristics of Arrays With Uniformly Illuminated Contiguous Subarrays

1. INTRODUCTION

A number of reasons exist for choosing to design large phased arrays with uniformly illuminated contiguous subarrays. Aside from the obvious simplicity of constructing an array of large, similar clusters of elements, contiguous subarray fabrication affords an economical means of introducing amplitude taper or time delay across an array. In addition, the use of phase shifters with discrete phase states leads to the formation of contiguous subarrays with a constant phase state or a phase progression across each subarray different from that for the array scan angle. In each of these occurrences, partitioning an array into subarrays gives rise to grating lobes caused by the periodic errors in the aperture illumination functions.

This short report presents several extremely simple approximate formulas for estimating the grating lobe levels of arrays with contiguous, uniformly illuminated subarrays. The formulas are sufficiently general to be applicable to most array factor illumination functions. Therefore, the results are presented in terms of array beam-broadening factors to retain this generality. Although the primary areas of concern are the grating lobes caused by stepwise approximation of amplitude taper (Figure 1B), and the use of time delay steering in combination with phased steered subarrays (Figure 1C), the report begins with a brief treatment of

(Received for publication 9 January 1984)

the grating lobes caused by phase quantization effects in a uniformly illuminated array (Figure 1A).

Shown to the right of Figures 1A, 1B, and 1C are representative curves for 64-element arrays, with $\lambda_0/2$ spacing between elements and 8 elements per subarray. In each case, the grating lobes resulting from subarray level pattern distortion are evident. The horizontal bars denoted at each grating lobe are the approximate grating lobe levels computed using the analysis in Section 2.

2. CHARACTERISTICS OF AN ARRAY OF UNIFORMLY ILLUMINATED CONTIGUOUS SUBARRAYS

Figure 1 shows the schematic organization of an array of uniformly illuminated contiguous subarrays. In the most general cases treated, there will be time delay devices and amplitude taper applied at the subarray input ports, but there will be, at most, phase shift $\Delta\phi$ between the elements within each subarray. The phase increment between elements required to scan the subarray to an angle θ_0 is

$$\Delta\phi = \frac{2\pi d}{\lambda_0} u_0 \tag{1}$$

where $u_0 = \sin \theta_0$, d is the element spacing, and λ_0 is the wavelength at the design frequency.

The normalized far field pattern of this array (neglecting the array element patterns) is given below for an array of $\mathcal{M}$ subarrays of M elements each.

$$F(u) = \frac{1}{\mathcal{M}} \sum_{q=-\left(\frac{\mathcal{M}-1}{2}\right)}^{\frac{\mathcal{M}-1}{2}} \omega_q \, e^{jqMz} \left[\frac{1}{M} \sum_{i=-\left(\frac{M-1}{2}\right)}^{\frac{M-1}{2}} e^{jiy} \right] \tag{2}$$

where

$$\sum_q |\omega_q| = \mathcal{M}$$

In this convention, the sums over i and q are over integers for M or $\mathcal{M}$ odd, and over half-integers for M or $\mathcal{M}$ even. The variables z and y are given by

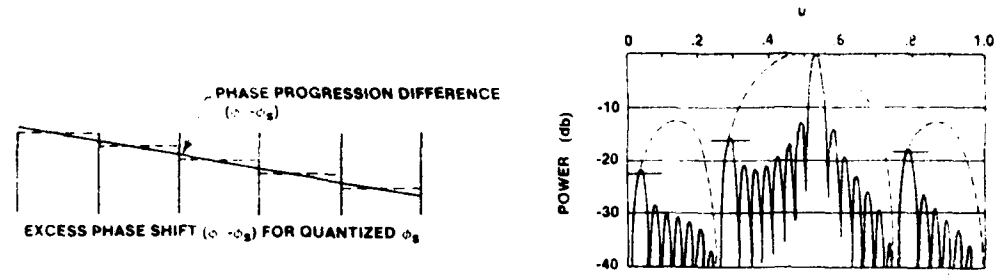

A. CASE 1: DISCRETE PHASE SHIFTER STATES (EQUAL AMPLITUDE WEIGHTS)

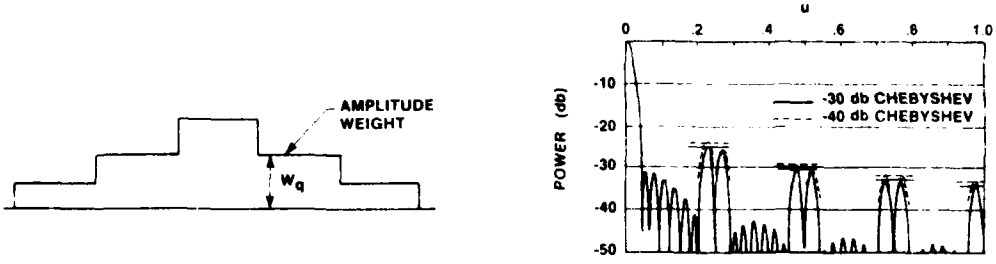

B. CASE 2: TAPER AT SUBARRAY PORTS (IDEAL PHASE PROGRESSION)

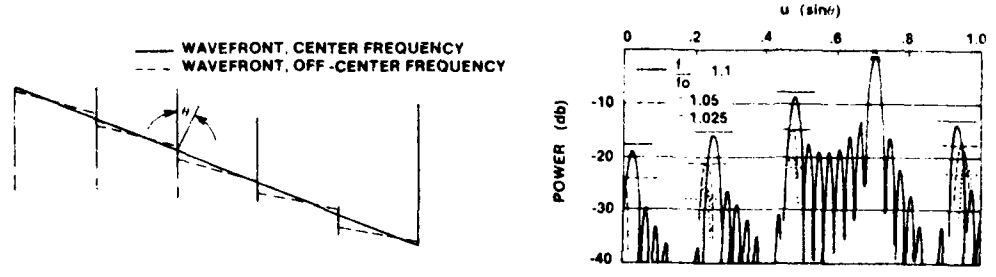

C. CASE 3: TIME DELAY AT SUBARRAY PORTS (EQUAL AMPLITUDE WEIGHTS)

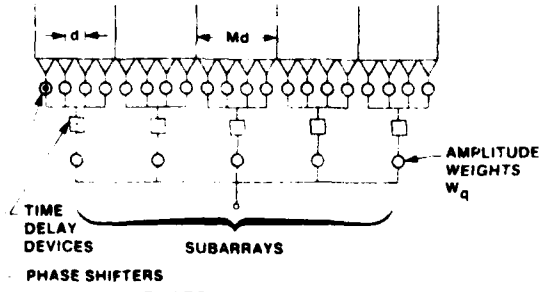

D. ARRAY OF CONTIGUOUS SUBARRAYS

Figure 1. Three Types of Contiguous Subarrays and Their Radiation Patterns. A. Case 1: Discrete Phase Shifter States (Equal Amplitude Weights). B. Case 2: Taper at Subarray Input Ports (Ideal Phase Progression). C. Case 3: Time Delay st Subarray Ports (Equal Amplitude Weights). D. Array of Contiguous Subarrays. Data are for 64-element arrays with $\lambda/2$ spacing between elements and 8 elements per subarray

$$z = \frac{2\pi d}{\lambda}(u - u_0);\quad u = \sin\theta \qquad \zeta = \frac{2\pi d}{\lambda}\,u - \Delta\phi \qquad (3)$$

$$u_0 = \sin\theta_0 \qquad = \frac{2\pi d}{\lambda}\left(\frac{u}{\lambda} - \frac{u_s}{\lambda_0}\right)$$

for the array with subarrays steered to u_s by phase shifters ($u_s \neq u_0$ in general), and with time delay between the subarray ports. Since all subarrays are the same size and have constant illumination, the pattern is obviously the product of an array factor $A(z)$ and a subarray pattern $f(\zeta)$, or

$$F(u) = A(z)f(\zeta) \qquad (4)$$

with the subarray pattern the bracketed expression of Eq. (1) summed to

$$f(\zeta) = \frac{\sin M\zeta/2}{M \sin \zeta/2} \qquad (5)$$

and the array pattern given in general as the remaining part of Eq. (2).

Since the subarrays will, in general, be several wavelengths across, grating lobes of the array factor $A(z)$ will occur at the direction cosines

$$u_p = u_0 + \frac{p\lambda}{Md};\quad p = (\pm 1, \pm 2 \ldots .) \qquad (6)$$

for all p corresponding to real space ($|u_p| < 1$).

Very simple and convenient estimates of the residual grating lobe levels are obtained by approximating the array factor and the subarray pattern in the vicinity of any "p'th" grating lobe by defining the variable δu so that

$$u = u_0 + \frac{p\lambda}{Md} + \delta u \qquad (7)$$

With this substitution, the parameters z and ζ become

$$z = 2\pi\left(\frac{d}{\lambda}\,\delta u + \frac{p}{M}\right) \qquad (8)$$

$$\zeta = 2\pi\left[\frac{d}{\lambda}\,\delta u + \frac{p}{M} + \frac{u_0}{\lambda_0}\left(\frac{\Delta f}{f_0}\right) + \frac{d}{\lambda_0}\,(u_0 - u_s)\right] \qquad (9)$$

where $\Delta f = f - f_0$ is the difference between the frequency and the design frequency f_0.

The coordinate δu is thus the angular displacement (in direction cosine space) from the p'th grating lobe. Note that for integer p, the array factor is exactly replicated in the vicinity of each lobe, or (for $|u| < 1$)

$$A(z) = A\left(\frac{2\pi d}{\lambda}\,\delta u\right)$$

The subarray pattern for this generalized case is given in terms of the localized coordinate δu as

$$f(y) = \frac{(-1)^p \sin\left[\pi M \frac{u_0}{\lambda_0}\,\frac{\Delta f}{f_0} + \frac{\pi d}{\lambda} M\,\delta u + \frac{\pi M d}{\lambda_0}(u_0 - u_s)\right]}{M \sin\left[\frac{\pi u_0}{\lambda_0}\,\frac{\Delta f}{f_0} + \frac{\pi p}{M} + \frac{\pi d}{\lambda}\,\delta u + \frac{\pi d}{\lambda_0}(u_0 - u_s)\right]} \tag{10}$$

Eq. (2) and Eq. (10) will be used to investigate the three special cases discussed in this report.

In each case, the methodology will be to use Eq. (10) for the subarray pattern and seek local expansions of the numerator, when appropriate, that describe behavior near grating lobe peaks. The accuracy of this analysis is greatest for cases in which the array factor beam is very narrow compared to the subarray beamwidth. In practice, this means that the results are applicable to arrays with six or more subarrays.

2.1 Case 1. Phase Quantization in a Uniformly Illuminated Array

An array excited by digitally quantized phase shifters is one example that can be analyzed as a subarraying problem. In Case 1, phase quantization in a uniformly illuminated array (Figure 1), the desired linear phase progression cannot be exactly maintained by phase shifters with phase progression having the least significant bit:

$$\delta = \frac{2\pi}{2^N} \tag{11}$$

To form a beam at u_0, the required incremental phase shift between elements is (at $\lambda = \lambda_0$)

$$\Delta\phi = \frac{2\pi d}{\lambda_0} \sin\theta_0 = \frac{2\pi d}{\lambda_0} u_0$$

Since the least significant bit is δ, the array can only be perfectly collimated at angles with required phase progression some multiple of δ. At any other scan angle, a phase progression that is some multiple of δ is applied to the array so that sections of the array have phase increment $(2\pi d/\lambda)\, u_s$ and point to some angle with direction cosine u_s. The remaining error in phase increment is $(2\pi d/\lambda) \cdot (u_s - u_0)$. This leads to an increasing error that can be corrected at various places across the array by inserting an added phase shift of the least significant bit (see Figure 1). The resulting pattern distortion takes its most serious form when the error buildup and its correction are entirely periodic, for then the array is divided into virtual subarrays, each subarray having the same phase error gradient. In this case, the distance between subarray phase centers is such that the total phase error increment between subarrays is equal to the phase of the least significant bit, or

$$|M\Delta\phi - M\Delta\phi_s| = \frac{2\pi d}{\lambda} M |(u_0 - u_s)| = \frac{2\pi}{2^N} \tag{12}$$

This expression is used to determine the subarray size M for specific $(u_0 - u_s)$ conditions.

The grating lobe level for this type of distortion is approximately the value of the subarray pattern at the grating lobe peaks ($\delta u = 0$). At center frequency, this is

$$|f(\vartheta)| = \left| \frac{\sin\left[M\frac{\pi d}{\lambda_0}(u_0 - u_s)\right]}{M \sin\left[\frac{\pi d}{\lambda_0}(u_0 - u_s) + \frac{p\pi}{M}\right]} \right| = \left| \frac{\sin\left[\pi/2^N\right]}{M \sin\left[\frac{\pi}{M2^N} + \frac{p'\pi}{M}\right]} \right| \tag{13}$$

The power of this grating lobe is written approximately

$$P_{g\ell} = |f|^2 = \left[\frac{\pi/2^N}{M \sin\left(\frac{p'\pi}{M}\right)} \right]^2 \tag{14}$$

where

$$p' = p + \frac{1}{2^N}$$

The factor $[M \sin (p\pi/M)]^{-2}$ is the envelope of the subarray pattern peak power sampled at the grating lobe point; this factor occurs in another expression given later, and so is plotted (in dB) in Figure 2 for valuesof $M > p$ (the near grating lobes). The general expression for power at the peak of the p'th grating lobe

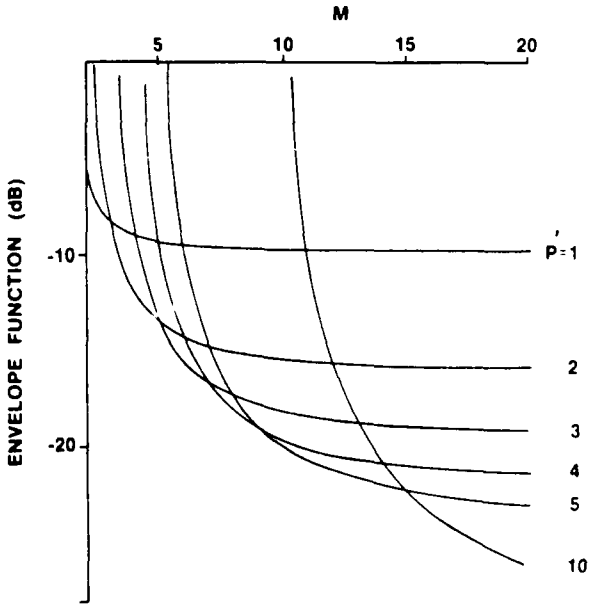

Figure 2. Envelope Factor (dB) vs Number of Elements in Subarray

[Eq. (14)] is thus obtained using this envelope function as

$$GL = 10 \log P_{g\ell} = \text{Envelope (dB)} + 20 \log \pi - 20N \log 2 = \text{Envelope (dB)} + 9.94 - 6.02N \quad (15)$$

Figure 1A shows a typical case of a uniformly illuminated 64-element array with $\lambda/2$ spacing. With 3-bit phase shifters (least bit 45°), the array forms a perfectly collimated beam at $u_s = u_0 = 0.5$ ($\theta_0 = 30°$), but at 32.1° ($u_0 = 0.53125$) with phase shifters set to the gradient inter-element phase $(2\pi d/\lambda)\, u_s$, there is an excess phase shift of 45° across each set of 8 elements. The pattern shows that grating lobes at various levels between 16 and 23 dB result from this periodic

phase error. The horizontal lines in the figure show the approximate grating lobe levels computed using Eq. (15). This figure also shows the subarray pattern of the 8-element subarray scanned to $u_s = 0.5$, and indicates how the product of subarray pattern and array factor limits the grating lobe heights.

Depending upon what scan angles are required, other size subarrays are formed at different scan angles. For example, at $u_0 = 0.5156$, $\theta = 31.04^\circ$, the excess of 45° phase shift spans 16-element subarrays. The grating lobe level in this case would turn out to be very close to that computed in Eq. (13) if the array were large enough, but an array of only 4 subarrays is not accurately represented by these approximate formulas. In this case, an error of several dB results from the direct use of Eq. (15).

In the limiting case of M large, the envelope curves tend to an asymptote, and the grating lobe power is

$$P_{g\ell} \doteq \left(\frac{1}{p'2^N}\right)^2 \tag{16}$$

of which a special case for $p = 1$ is the $P_{g\ell} = 1/2^{2N}$ result obtained by Miller,[1] using a different approach that is quoted in many standard texts.

2.2 Case 2. Amplitude Taper at Subarray Input Ports

A phase steered array, organized into equally spaced, uniformly illuminated subarrays, has its grating lobes located at the null points of the subarray pattern. If the array is uniformly excited, its beamwidth is narrow and the subarray nulls completely remove the grating lobes. When the excitation amplitude at the subarray input ports is weighted for array factor sidelobe reduction, the beamwidth broadens, and, at the grating lobe points, split (monopulse-like) beams as shown in Figure 1B occur.

To evaluate the power level of these split grating lobes, it is convenient to use a fairly general representation of the array factor [Eq. (2)] in the vicinity of each p'th grating lobe. At center frequency, and with each subarray scanned to θ_0 ($\Delta f = 0$; $\theta_s = \theta_0$), the array factor grating lobe is centered on the subarray pattern null, and, in the localized region from the beam peak out beyond the -3 dB point, can be approximated at each p'th grating lobe by the expression at

---

1. Miller, C.J. (1964) Minimizing the effects of phase quantization errors in an electronically scanned array, Proc. 1964 Symposium on Electronically Scanned Array Techniques and Applications, RADC-TDR-64-225, 1:17-38, RADC, Griffiss AFB, New York.

$$A(u) = \frac{B \sin\left[\frac{M\mathcal{M}\pi d}{B\lambda_0}\,\delta u\right]}{M\mathcal{M}\pi\frac{d}{\lambda_0}\,\delta u} \tag{17}$$

that represents a broadened beam with beam broadening factor B, that has been normalized to unity.

The beam broadening factor B is defined as follows:

(1) with reference to the half power beamwidth of a uniformly illuminated array of $\mathcal{M}$M elements spaced "d" apart, and

(2) so that the beamwidth is given approximately by $0.886\,\lambda_0 B/M\mathcal{M}d$, with B the ratio of the beamwidth of the tapered array to that of the uniformly illuminated array.

The subarray pattern for this case is given by Eq. (10) with $u_s = u_0$ and $\Delta f = 0$. For arrays with more than 4 subarrays, the grating lobe is so narrow that the sine in the numerator of 10 is approximated by its argument. In this case, Eq. (10) is written as

$$f(_z) = \frac{(-1)^p \left[M\pi\frac{d}{\lambda_0}\,\delta u\right]}{M \sin\left(\frac{p\pi}{M}\right)} \tag{18}$$

Near the p'th grating lobe, the product of the subarray pattern and the array factor is thus approximately

$$A(z)f(_z) = \frac{(-1)^p B \sin\left[\frac{\mathcal{M}M\pi}{B}\frac{d}{\lambda_0}\,\delta u\right]}{\mathcal{M}M \sin\left(\frac{p\pi}{M}\right)} \tag{19}$$

This expression has the proper zero at $\delta u = 0$ to produce the characteristic split lobe centered on the p'th grating lobe.

The normalized power at this grating lobe has the particularly simple form

$$P_{gl} = \frac{B^2}{\mathcal{M}^2 M^2 \sin^2\left(\frac{\pi p}{M}\right)} \tag{20}$$

indicating that the lobe value increases in proportion to the square of the array beamwidth but is restricted in size by the envelope of the subarray power pattern.

The grating lobe level can again be obtained from the envelope pattern (Figure 2) using

$$GL = 10 \log P_{gl} = \text{Envelope (dB)} + 20 \log B - 20 \log \mathcal{M} \tag{21}$$

Figure 1B shows an example of a 64-element array with $\lambda/2$ spacing grouped into eight contiguous subarrays and illuminated at the subarray input ports by -30 and -40 Chebyshev tapers. The figure reveals the split grating lobe characteristic mentioned earlier, but shows the lobes as clearly dominating the far sidelobe pattern. Based on beam broadening factors of 2.21 and 3.11 for the Chebyshev patterns, evaluation of Eq. (19) shows that the -40 dB pattern should have grating lobes about 0.9 dB higher than the -30 dB pattern. The computed levels [Eq. (21)] of Figure 1B obviously agree very closely with the computed pattern.

Eq. (21) is a good approximation for all beam broadening values, even the limiting case of uniform illumination (B = 1) where the grating lobe itself disappears. In this case of a uniformly illuminated array, Eq. (19) (using B = 1) gives the envelope of the sidelobe pattern at the grating lobe points for an arbitrary subdivision of the array. For example, one could consider the uniformly 64-element array to be eight groups of 8 elements, four groups of 16, etc., but, in each case, Eq. (11) will give the approximate sidelobe envelope at the grating lobe locations even though there are no grating lobes.

Finally, although this analysis has addressed the effects of amplitude taper assuming perfect phase quantization, the primary result of amplitude taper at the subarray input ports is to broaden the array main and grating lobe beamwidths. Therefore, the results given in Case 1 (Section 2.1) and Case 3 (Section 2.3) are valid approximations with or without amplitude taper.

2.3 Case 3. Time Delay at Subarray Ports

In the limit of very small frequency excursion for a large array, it may still be advantageous to use time delay at the subarray input ports.

In this case, the grating lobe peak is not split, and the peak grating lobe values are given directly by the subarray pattern envelope, as in Case 1 (Section 2.1).

Using a small angle expansion for the numerator of 10, the normalized power in the p'th lobe is

$$P_s = \frac{\pi^2 X^2}{\sin^2 \pi \left[X + p/M\right]} \quad \text{where } X = \frac{u_0 d}{\lambda_0} \frac{\Delta f}{f_0} \tag{22}$$

Note that $|X| < 1/M$, so that the main beam does not "squint" out to a grating lobe location. This insures that P_s never becomes singular.

A plot of grating lobe level vs the variable X is given in Figure 3 for various P/M ratios.

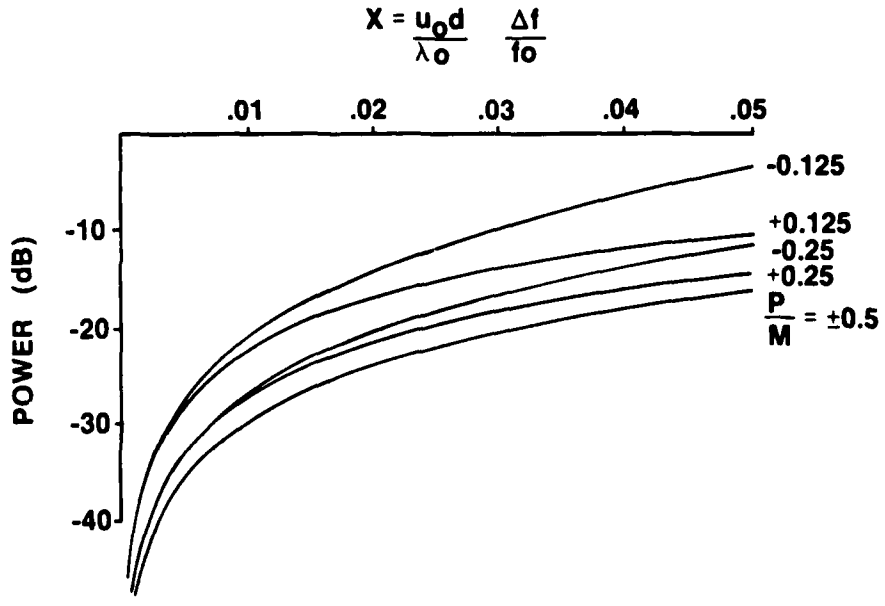

Figure 3. Grating Lobe Power for Array With Time Delay at Subarray Ports

Figure 1C shows an example of a uniformly illuminated array with time delay steering at the subarray level. The results of Eq. (22) are plotted as horizontal lines, and are clearly quite good representations of the computed grating lobe levels for various f/f_0 ratios.

3. CONCLUSION AND COMMENTS ABOUT GENERALITY

Figure 4 shows the grating lobe structure of a 64-element array with a -40 dB Chebyshev illumination at the input ports of 8-element subarrays. The array is scanned using time delay at the subarray input ports and phase shifters within the

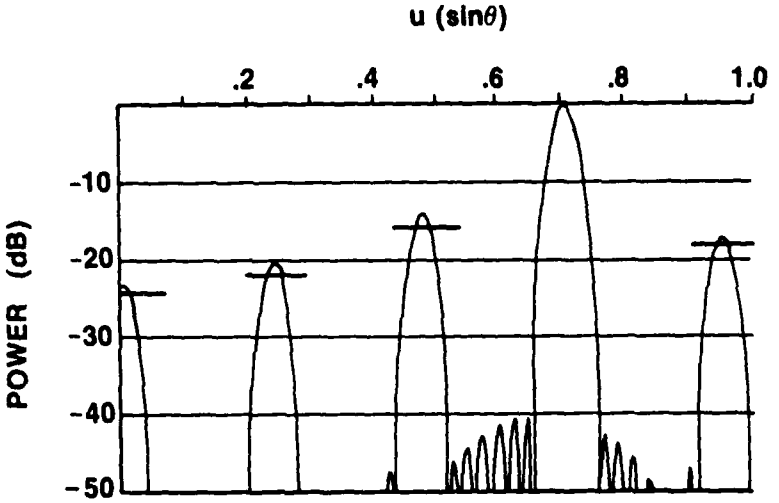

Figure 4. Power Pattern for Array With Time Delay at Subarray Ports and a 40 dB Chebyshev Taper $f/f_0 = 1.05$

subarrays. The solid horizontal lines show the grating lobe levels computed using Eq. (22) (or Figure 3) with $f/f_0 = 1.05$. The figure clearly indicates that the results for Case 3 can be extended to include a situation when there is pattern distortion caused by quantized amplitude taper in addition to time delay. The reason for this more general result is that Eq. (22) was derived on the basis of the subarray pattern envelope; since the subarray pattern null does not fall at the grating lobe point, the lobes are not split, and the beam broadening factor argument used in Case 2 does not apply. Therefore, if the grating lobes that result from Case 1- and Case 3-type distortion are large, then the grating lobes are sampling subarray pattern envelopes quite far from the nulls, and the quantized amplitude taper has little effect on the validity of the approximations. The Case 1 and Case 3 results can thus be applied in most situations even when the amplitude taper is quantized.

The results of this brief analysis are simple approximate formulas and graphs to predict the levels of grating lobes caused by various subarray excitations for arrays of contiguous subarrays. The scale of the graphs has been kept as general as possible to cover the widest possible range of array excitations.

MISSION
of
Rome Air Development Center

RADC plans and executes research, development, test and selected acquisition programs in support of Command, Control Communications and Intelligence (C^3I) activities. Technical and engineering support within areas of technical competence is provided to ESD Program Offices (POs) and other ESD elements. The principal technical mission areas are communications, electromagnetic guidance and control, surveillance of ground and aerospace objects, intelligence data collection and handling, information system technology, ionospheric propagation, solid state sciences, microwave physics and electronic reliability, maintainability and compatibility.

Printed by
United States Air Force
Hanscom AFB, Mass. 01731


DATE
ILME